

Pion Structure as Observed in the Reaction $\pi^- N \rightarrow \mu^+ \mu^- X$ at 80 GeV/c

S. Palestini,^(a) C. Biino, J. F. Greenhalgh,^(b) W. C. Louis, K. T. McDonald, F. C. Shoemaker,
and A. J. S. Smith

Joseph Henry Laboratories, Princeton University, Princeton, New Jersey 08544

C. E. Adolphsen,^(c) J. P. Alexander,^(d) K. J. Anderson, J. S. Conway, J. G. Heinrich,
K. W. Merritt,^(e) and J. E. Pilcher

Enrico Fermi Institute and Department of Physics, The University of Chicago, Chicago, Illinois 60637

and

E. I. Rosenberg and D. T. Simpson^(f)

Ames Laboratory and Department of Physics, Iowa State University, Ames, Iowa 50011

(Received 19 September 1985)

The production of $\mu^+ \mu^-$ pairs with large longitudinal momentum has been studied in $\pi^- N$ collisions. The data confirm an earlier result that most of the pair production takes place via longitudinally polarized virtual photons as $x_F \rightarrow 1$. The transverse-momentum distribution of the muon pairs shows a marked narrowing in the same limit. The distribution of valence quarks in the pion is extracted, and indicates a nonzero probability of having a single quark carry all available longitudinal momentum. These results are compared with a QCD model of pion structure which includes the effect of higher-twist corrections.

PACS numbers: 13.85.Qk, 14.40.Aq

After the first observation of a continuum of $\mu^+ \mu^-$ pairs produced in pN collisions,¹ the mechanism for this process was suggested to be the annihilation of a quark and an antiquark to a virtual photon.² This possibility allows one to explore the distribution of quarks in both the beam and target particles, and hence study the structure of any long-lived hadron. In a previous experiment we made the first measurement of the structure function of the pion by this technique.³ Supporting evidence for the applicability of the quark-antiquark annihilation model in πN collisions comes from comparison of $\pi^+ C$ and $\pi^- C$ cross sections,^{4,5} observation of a $1 + \cos^2 \theta$ decay angular distribution for the muon pairs,⁵ approximate validity of the $M^3 d\sigma/dM$ scaling law,⁶ and A^1 dependence of the cross section on the atomic number of the nuclear target.⁷

In a previous experiment⁸ we found an indication that muon pairs which carry away a large fraction of the incident pion momentum appear to have been produced via photons with longitudinal rather than transverse polarization. This was anticipated in a view of the quark-antiquark annihilation in which the quarks contributing to this kinematic region are not free particles but are subject to bound-state ("higher-twist") effects.⁹ However, the result was not confirmed in a subsequent experiment.¹⁰ According to the concept of asymptotic freedom, effects associated with initial-state masses will not survive at large center-of-mass energies. Hence any longitudinal polarization of the virtual photon is likely related to a "scale-breaking" effect, as is indeed explicitly predict-

ed in Ref. 9.

To clarify these issues we have performed a new experiment on the forward production of muon pairs in πN collisions. The goal was a detailed investigation of the kinematic region in which most of the momentum of the pion is transformed into that of the muon pair. To search for scale-breaking effects the experiment was performed with 80- and 255-GeV/c beam momenta, chosen to allow comparison of continuum muon-pair production at values of the scaling variable $\tau = M^2/s \sim 0.1$. This Letter reports first results from the 80-GeV/c data sample only.

The apparatus is described in considerable detail elsewhere.¹¹ The 80-GeV/c pion beam was incident on a tungsten target which preceded a double-magnet spectrometer. The first magnet prepared high-mass muon pairs for efficient recognition by a hardware trigger processor, and also absorbed secondary hadrons in low- Z material. The main portion of the detector was a conventional charged-particle spectrometer based on a large-aperture dipole magnet surrounded by multiwire proportional chambers and drift chambers. In a run of some 7.2×10^{13} incident pions we collected about 4×10^7 triggers of which 4060 were reconstructed as $\mu^+ \mu^-$ pairs with $M > 4$ GeV/c.^{2,12}

The acceptance of the spectrometer was broad in all kinematic variables describing the muon pairs. However, muons of less than 10-GeV/c momentum could not penetrate the hadron absorbers, and so the acceptance was restricted to pairs of $x_F > 0.15$, where x_F (Feynman x) is the fraction of available longitudinal momentum. Correspondingly, the *high-mass* muon

pairs with $M > 4 \text{ GeV}/c^2$ were produced only from antiquarks with fraction $x_\pi > 0.4$ of the momentum of the pion. [These variables are related by $x_F = (x_\pi - x_N)/(1 - \tau)$; $x_\pi x_N = \tau$, where x_N is the momentum fraction carried by the annihilating quark in a nucleon.] The resolution in the various reconstructed parameters of the muon pairs was limited primarily by multiple scattering in the tungsten target and the spread in incident pion momentum. Typical values for the rms reconstruction errors were $0.14 \text{ GeV}/c^2$ for mass M , 0.04 for x_F , 0.03 for x_π , 0.04 for x_N , $0.13 \text{ GeV}/c$ for P_T , and 0.06 for $\cos\theta_t$.

We have fitted the angular distribution of the muons in the muon-pair rest frame with the form $1 + \lambda \cos^2\theta$. We find $\lambda = 0.64 \pm 0.13$ for θ measured with respect to the t -channel axis and $\lambda = 0.66 \pm 0.17$ using the Collins-Soper axis,¹³ integrating over all *high-mass* pairs. Of greater interest is the dependence of parameter λ on x_π as shown in Fig. 1 for the t channel. At large x_π the angular distribution approaches the form $\sin^2\theta_t$, which is model-independent evidence of longitudinal polarization of the virtual photon, as previously reported.⁸

We have also compared the data to the most general form of the angular distribution for lepton-pair production via a virtual photon¹⁴:

$$\frac{d\sigma}{d\Omega} \propto 1 + \lambda \cos^2\theta + \rho \sin 2\theta \cos\phi + \omega \sin^2\theta \cos 2\phi.$$

The statistical power of the fit is limited by the size of the data sample. We find no significant departures of parameters ρ and ω from zero in any region of x_π , but these parameters are also consistent with the slightly nonzero values suggested in model calculations.⁹

Additional evidence for modifications to muon-pair production at large longitudinal momentum comes from the transverse momentum of the pairs. To minimize the effect of reduction of transverse phase space for high longitudinal momentum, we define Feynman x in the center-of-mass frame as $x_F = P_L/P_L^{\text{max}}$ where

$$P_L^{\text{max}} = \frac{\sqrt{s}}{2} \left[1 - 2 \frac{M^2 + M_R^2}{s} + \frac{(M^2 - M_R^2)^2}{s^2} - \frac{4P_T^2}{s} \right]^{1/2}.$$

We take the mass of the recoiling system, M_R , to be $0.94 \text{ GeV}/c^2$. Our definition of P_L^{max} distributes uniformly in x_F the reduction of phase space which occurs at high P_T . The results for $\langle P_T \rangle$ and $\langle P_T^2 \rangle$ are displayed in Fig. 2 as functions of x_F . The value of $\langle P_T^2 \rangle \sim 1.0 \text{ GeV}/c$ at moderate x_F is in good agreement with the trend of $\langle P_T^2 \rangle$ vs s observed in other muon-pair production experiments.¹⁵ The average transverse momentum drops dramatically at large x_F , in roughly the same region that the angular distribution changes its character.

Information as to the structure of the pion, and of the target nucleons, was extracted from the observed muon-pair cross section according to the model of quark-antiquark annihilation:

$$\frac{d^2\sigma}{dx_\pi dx_N} = K \frac{4\pi\alpha^2}{9s\tau^2} \sum_q e_q^2 x_\pi x_N [q_\pi(x_\pi) \bar{q}_N(x_N) + \bar{q}_\pi(x_\pi) q_N(x_N)].$$

Here $q(x)$ is the probability of finding a quark carrying momentum fraction x of its parent hadron,¹⁶ and K is an overall normalization factor representing the net effect of a large class of higher-order QCD corrections.¹⁷ Our acceptance was restricted to the region $x_\pi > 0.4$, where only the valence quark distributions of the pion are significant. Taking note of G -parity invariance, we define the structure function of the pion as

$$F_\pi(x_\pi) = x_\pi \bar{u}_{\pi^-}^v(x_\pi) = x_\pi d_{\pi^-}^v(x_\pi),$$

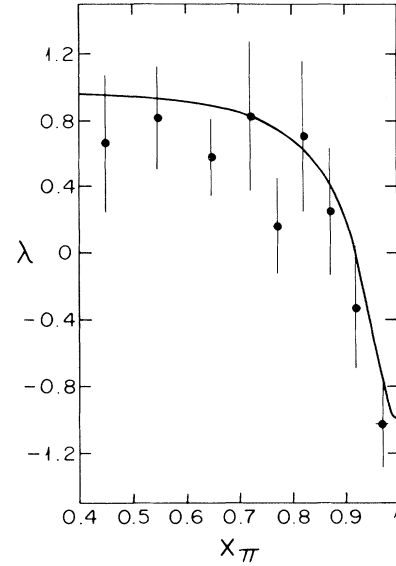


FIG. 1. The parameter λ as a function of x_π obtained from fits to the angular distribution of the muons in the muon-pair rest frame, using the form $d\sigma/d\cos\theta \propto 1 + \lambda \cos^2\theta$, where θ measures the μ^+ direction with respect to the t -channel axis. The solid curve is based on the QCD model of Berger and Brodsky (Ref. 9) with the value $\langle k_T^2 \rangle = 0.62 \text{ GeV}^2/c^2$ deduced from the observed pion structure function.

where the superscript v indicates a valence quark. Then the annihilation cross section simplifies to the expression

$$\frac{d^2\sigma}{dx_\pi dx_N} = K \frac{4\pi\alpha^2}{9s\tau^2} F_\pi(x_\pi) F_N(x_N),$$

where we have introduced an effective structure function for the tungsten nucleus

$$F_N(x_N) = x_N \left\{ \frac{4}{9} [0.4u_p^v(x_N) + 0.6d_p^v(x_N)] + \frac{5}{9} S_p(x_N) \right\}.$$

In F_N the distributions u_p^v , d_p^v , and S_p are for the valence u quarks, the valence d quark, and the sea quarks of the proton, respectively, and the coefficients 0.4 and 0.6 arise from the relative proton and neutron content of tungsten nuclei.

To use the above formalism the *high-mass* muon-pair events ($M > 4 \text{ GeV}/c^2$ and $x_F > 0.15$) were binned into cells of size $\Delta x_\pi = 0.05$ by $\Delta x_N = 0.025$. A total of 143 cells were populated, labeled by twelve values of x_π from 0.4 to 1.0, and sixteen values of x_N from 0.1 to 0.5. A fit was made with the cross section $d^2\sigma/dx_\pi dx_N$, taking as parameters the values of the pion structure function F_π at the centers of the twelve x_π bins and the values of the nucleon structure function F_N at the centers of the sixteen bins of x_N . The χ^2 value for the fit was 123 for 116 degrees of freedom, indicating good consistency for a factorized form of the cross section. The residuals between the fit and the 143 cell contents showed no excessive contribution to the χ^2 from any region on the (x_π, x_N) grid. The fit values for the pion structure function are shown as points with error bars in Fig. 3, in arbitrary units.

We have parametrized the pion structure function as

$$F_\pi(x_\pi) \propto x_\pi^\alpha [(1-x_\pi)^\beta + \gamma].$$

This form permits a finite intercept, γ , at $x_\pi = 1$ as suggested in various models.^{9,18} Table I gives the results of four fits by $d^2\sigma/dx_\pi dx_N$ using the above functional form for F_π . In fits *a-c* the nucleon structure function was fixed at the values obtained in the

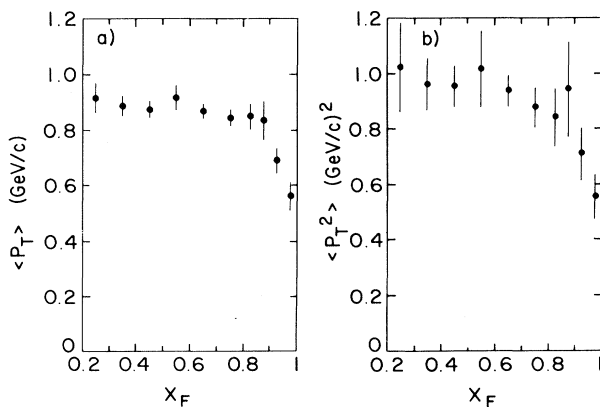


FIG. 2. (a) The average transverse momentum and (b) the average squared transverse momentum of the muon pairs as functions of Feynman x .

factorized fit with the cross section described above, while in fit *d*, F_N was taken from previous measurements of the quark distributions in the nucleon.¹⁹ The stated errors are statistical only. The inset in Fig. 3 shows the high- x_π region of the pion structure function superimposed with fits *a* and *b*.

We have explored various systematic influences on the magnitude of the intercept γ . With data only for $x_\pi > 0.4$ the parameter α could not be well determined, and so in fit *c* it was set equal to 0.4, a value found in a previous experiment with greater acceptance in the low- x_π region.²⁰ This is seen to have little effect on parameter γ . The analysis near $x_\pi = 1$ is sensitive to the value of the pion beam momentum, which was measured by two different methods with a consistency of 0.5 GeV/c.¹¹ If we increase the beam momentum assumed in the analysis by this amount, parameter γ is reduced by 0.0015 for fit *b* and by 0.0020 for fit *c*. The true value of x_π is also affected by the smearing of the center-of-mass energy due to Fermi motion. As a measure of this, if we omit the Fermi-motion correction in the acceptance calculation the value of γ is reduced by 0.0007.

The nucleon structure function that we measure is somewhat steeper than that found in lepton-hadron

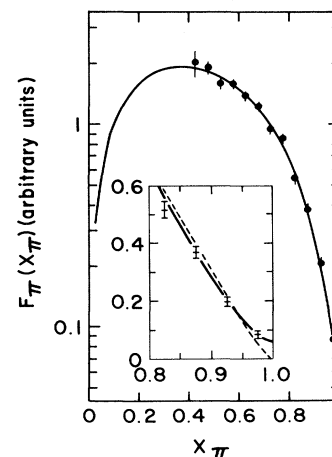


FIG. 3. The twelve fitted values for the pion structure function, in arbitrary units. The solid curve is the functional fit *b* described in the text. The insert shows the large- x_π region of the pion structure function. The solid curve is again fit *b* while the dashed curve is from fit *a*.

scattering experiments with nuclear targets,¹⁹ but this has little effect on the pion structure function, as illustrated by comparison of fits *b* and *d*. If we use F_N taken from Ref. 19, the parameters β and γ of the fit to the high- x_π region of the pion structure function are altered by less than 1 standard deviation.

We do not make a measurement of the factor K as this would require a large extrapolation from our data, which lie below $x_\pi = 0.4$.

Our several results on forward muon-pair production in πN collisions are consistent with the predictions of the QCD model of Berger and Brodsky.⁹ They suggest that for $x_\pi > 0.5$,

$$\frac{d^2\sigma}{dx_\pi d\cos\theta} \propto x_\pi \left[(1-x_\pi)^2(1+\cos^2\theta) + \frac{4}{9} \frac{\langle k_T^2 \rangle}{M^2} \sin^2\theta \right],$$

where $\langle k_T^2 \rangle$ is the average squared intrinsic transverse momentum of the annihilating quarks. On integration over angles this becomes

$$\frac{d\sigma}{dx_\pi} \propto F_\pi(x_\pi) \propto x_\pi \left[(1-x_\pi)^2 + \frac{2}{9} \frac{\langle k_T^2 \rangle}{M^2} \right].$$

Our best fit for the pion structure function (fit *b* of Table I) for $x_\pi > 0.4$ lies closer to this prediction than earlier work^{3,6,20} which placed greater emphasis on the low- x_π region. The result $\gamma = 0.0060 \pm 0.0016$ corresponds to a value of the intrinsic transverse momentum of $\langle k_T^2 \rangle = 0.62 \pm 0.16 \text{ GeV}^2/c^2$ (with $\langle M^2 \rangle = 23 \text{ GeV}^2/c^4$), which agrees well with the observed dip in $\langle P_T^2 \rangle$ at large x_F to $0.56 \pm 0.08 \text{ GeV}^2/c^2$. Inserting $\langle k_T^2 \rangle = 0.62 \text{ GeV}^2/c^2$ into the predicted expression for $d^2\sigma/dx_\pi d\cos\theta$, we calculate the parameter λ as a function of x_π to be the solid curve in Fig. 1.

Additional tests of the QCD predictions will be possible when we have completed the analysis of the 60 000 high-mass muon pairs collected with a 255-GeV/c pion beam. Analysis of a subsample of that data,²¹ comparable in size to that described here, lends quantitative support to the conclusions of this Letter.

We wish to thank the electronic and engineering support staffs of our institutions for their part in the construction of the apparatus. The staff at Fermilab deserves special thanks for the large effort which made the experiment possible during the initial operation of the superconducting accelerator. This work was supported in part by the U.S. Department of Energy under Contracts No. DE-AC02-76ER03072 and No. W-7405-ENG-82-KA-01-01 and by the National Science Foundation.

(a) Present address: Istituto Nazionale di Fisica Nucleare, Sezione di Torino, Torino, Italy.

(b) Present address: Fonar Corp., Melville, N.Y. 11747.

(c) Present address: University of California at Santa Cruz, Santa Cruz, Cal. 95064.

(d) Present address: SLAC, Stanford, Cal. 94305.

TABLE I. Functional fits to the pion structure function.

Fit	α	β	γ	$\chi^2/\text{d.o.f.}$
<i>a</i>	0.05 ± 0.54	1.12 ± 0.18	0, fixed	138/126
<i>b</i>	0.92 ± 0.38	1.59 ± 0.18	0.0060 ± 0.0016	130/125
<i>c</i>	0.4, fixed	1.37 ± 0.07	0.0072 ± 0.0021	132/126
<i>d</i>	1.58 ± 0.35	1.72 ± 0.16	0.0049 ± 0.0012	192/140

(e) Present address: Fermilab, Batavia, Ill. 60510.

(f) Present address: IBM, Endicott, N.Y. 13760.

¹J. H. Christenson *et al.*, Phys. Rev. Lett. **25**, 1523 (1970).

²S. D. Drell and T.-M. Yan, Phys. Rev. Lett. **25**, 316, 902(E) (1970), and Ann. Phys. **66**, 578 (1971).

³C. B. Newman *et al.*, Phys. Rev. Lett. **42**, 951 (1979).

⁴J. G. Branson *et al.*, Phys. Rev. Lett. **38**, 1334 (1977).

⁵G. E. Hogan *et al.*, Phys. Rev. Lett. **42**, 948 (1979).

⁶R. Barate *et al.*, Phys. Rev. Lett. **43**, 1541 (1979).

⁷J. Badier *et al.*, Phys. Lett. **104B**, 335 (1981); H. J. Frisch *et al.*, Phys. Rev. D **25**, 2000 (1982).

⁸K. J. Anderson *et al.*, Phys. Rev. Lett. **43**, 1219 (1979).

⁹E. L. Berger and S. J. Brodsky, Phys. Rev. Lett. **42**, 940 (1979); E. L. Berger, Z. Phys. C **4**, 289 (1980).

¹⁰J. Badier *et al.*, Z. Phys. C **11**, 195 (1981).

¹¹C. Biino *et al.*, to be published.

¹²For details of the analysis see S. Palestini, Ph.D. dissertation, Princeton University, 1984 (unpublished).

¹³J. C. Collins and D. E. Soper, Phys. Rev. D **16**, 2219 (1977).

¹⁴R. C. Oakes, Nuovo Cimento **44A**, 440 (1966).

¹⁵J. Badier *et al.*, Phys. Lett. **117B**, 372 (1982).

¹⁶In general, the quark probability distributions $q(x)$ are also functions of such variables as the invariant mass and the transverse momentum of the muon pair. The size of the data sample of the present experiment does not permit detailed study of this functional dependence, and we report structure functions which are averaged over all variables except the longitudinal momentum of the quark.

¹⁷See for example, J. Ellis, in *Proceedings of the Ninth International Symposium on Lepton and Photon Interactions at High Energies, Batavia, Illinois, 1979*, edited by T. B. W. Kirk and H. D. I. Abarbanel (Fermilab, Batavia, Ill., 1980).

¹⁸S. D. Drell, D. J. Levy, and T.-M. Yan, Phys. Rev. D **1**, 1617 (1970); P. V. Landshoff and J. C. Polkinghorne, Nucl. Phys. **B53**, 473 (1973); Z. F. Ezawa, Nuovo Cimento **23A**, 271 (1974); G. R. Farrar and D. R. Jackson, Phys. Rev. Lett. **35**, 1416 (1975); R. D. Field and R. P. Feynman, Phys. Rev. D **15**, 2590 (1977).

¹⁹J. G. H. de Groot *et al.*, Phys. Lett. **82B**, 456 (1979), and Z. Phys. C **1**, 143 (1979).

²⁰J. Badier *et al.*, Z. Phys. C **18**, 281 (1983).

²¹J. P. Alexander *et al.*, to be published.